

STRUCTURE ELUCIDATION OF NATIVE N- AND O-LINKED GLYCANS BY TANDEM MASS SPECTROMETRY (TUTORIAL)

Hyun Joo An^{1,2} and Carlito B. Lebrilla^{1,2*}

¹Department of Chemistry, University of California, Davis, CA 95616

²Department of Biochemistry and Molecular Medicine, University of California, Davis, CA 95616

Published online 22 November 2010 in Wiley Online Library (wileyonlinelibrary.com). DOI 10.1002/mas.20283

Oligosaccharides play important roles in many biological processes. However, the structural elucidation of oligosaccharides remains a major challenge due to the complexities of their structures. Mass spectrometry provides a powerful method for determining oligosaccharide composition. Tandem mass spectrometry (MS) provides structural information with high sensitivity. Oligosaccharide structures differ from other polymers such as peptides because of the large number of linkage combinations and branching. This complexity makes the analysis of oligosaccharide unique from that of peptides. This tutorial addresses the issue of spectral interpretation of tandem MS under conditions of collision-induced dissociation (CID) and infrared multiphoton dissociation (IRMPD). The proper interpretation of tandem MS data can provide important structural information on different types of oligosaccharides including O- and N-linked. © 2010 Wiley Periodicals, Inc., *Mass Spec Rev* 30:560–578, 2011

Keywords: N-glycan; O-glycan; structure; tandem mass spectrometry; CID; IRMPD

I. INTRODUCTION

A. Background

Glycosylation is one of the most common post-translational modifications of proteins whereby glycans are added to the protein chain (Apweiler, Hermjakob, & Sharon, 1999). These oligosaccharides play key roles in a number of cell–cell recognition processes (Varki, 1993) including immunity (Rudd et al., 2001), infection (Dube & Bertozzi, 2005; Cooke et al., 2007), and may provide important biological markers for a wide variety of diseases (An et al., 2005; Fuster & Esko, 2005; An et al., 2006; Kirmiz et al., 2007). There has previously been a lack of analytical tools for the structural elucidation of oligosaccharides creating a barrier toward understanding structure–function relationships of this important class of compounds. Unlike peptides or oligonucleotides, oligosaccharide structures are further complicated by the presence of stereoisomers, numerous connectivities, and branching. However, recent developments particularly in mass spectrometry (MS) have produced new techniques that are highly sensitive while providing structural information.

Tandem MS has been applied to the structural interrogation of an increasing number of biomolecules including oligosac-

charides (Harvey, 2005; Zhang et al., 2005; Hitchcock et al., 2008), peptides (Ishihama, 2005; Chen & Pramanik, 2008), and glycopeptides (Wuhrer et al., 2007; Seipert et al., 2008). Tandem MS (MSⁿ) involves the isolation of specific ion species that are further probed for structures. Tandem MS methods are ideal for oligosaccharide analysis. Oligosaccharide from biological samples can be readily separated and analyzed with minimal separation prior to ionization because the ion of interest can be isolated and probed individually in the gas phase. Tandem MS may require only picograms of material; however, there is a wealth of information available within a set of MSⁿ spectra. Linkage as well as branching is often accessible by tandem MS. However, elucidating structures based on tandem MS remains far from routine. While there have been attempts to annotate structure based on tandem MS, they typically provide partial structures (Lohmann & von der Lieth, 2004; Ceroni et al., 2008). Furthermore, there is still no universal software for the automatic interpretation of mass spectra primarily because of heterogeneity and structural diversity in oligosaccharides.

There are many methods of tandem MS; however, they can all be classified into essentially two groups based on the method of energy deposition—vibrational and electronic. The former includes low energy collision-induced dissociation (CID) and infrared multiphoton dissociation (IRMPD), whereas the latter includes high energy CID, electron capture dissociation (ECD), electron transfer dissociation (ETD), and UV photodissociation.

This tutorial is not meant to be a comprehensive review on oligosaccharide analysis. There are already extensive reviews in this area (Park & Lebrilla, 2005; Harvey, 2006, 2008). Instead, this tutorial aims to aid the reader with the interpretation of tandem MS data for the elucidation of structures of oligosaccharides. We illustrate how to interpret the tandem mass spectra obtained from high/low-energy CID and IRMPD. The IRMPD and CID behavior of oligosaccharides is more specifically compared. The mechanisms by which the glycans undergo fragmentation in the tandem mass analysis are also discussed in light of interpreting tandem MS spectra.

B. N- and O-Linked Glycans

The large diversity of oligosaccharides makes a general discussion of all types of oligosaccharides and their glycoconjugates difficult. This tutorial is focused on N- and O-linked glycans. Other oligosaccharides such as those found in specific glycoconjugates, including glycolipids and peptidoglycans, have their own distinct fragmentation behavior. Furthermore, highly anionic oligosaccharides such as the glycosaminoglycans and the polysialic acids require specific chemical methods of pretreatment and specific methods for activation to obtain useful structural information (Zaia & Costello, 2003; Chi, Amster, &

*Correspondence to: Carlito B. Lebrilla, Department of Chemistry, University of California, One Shields Avenue, Davis, CA 95616.
E-mail: cblebrilla@ucdavis.edu

Linhardt, 2005; Didraga, Barroso, & Bischoff, 2006; Wolff et al., 2007).

O-linked glycans are linked to a serine or threonine of the polypeptide backbone. There is no consensus sequence for O-linked glycans, but they are generally found in serine and threonine-rich regions of proteins. Mucins are very large glycoproteins that are highly glycosylated. For this reason, O-linked glycans are sometimes referred to as mucin-type oligosaccharides. O-linked glycans are generally smaller (compared to N-linked glycans) consisting of 3–10 monosaccharide residues. There are a number of core structures and as many as eight have been reported (Brockhausen, 1999) (Fig. 1).

N-linked glycans are found on an asparagine as part of a three-amino-acid consensus sequence NXS/T, where X is any amino acid except proline and the third amino acid can be serine (S) or threonine (T). All N-linked glycans are derived from the precursor $\text{Glc}_3\text{Man}_9\text{GlcNAc}_2$, which is attached to the protein during translation. The precursor is subjected to various modifications in the Golgi and in the endoplasmic reticulum (ER). The modification can result in three types of glycan structures—high mannose, complex, and hybrid (Fig. 2b). These oligosaccharides are generally larger (typically 10–20 monosaccharide residues) with a single common core (Fig. 2a). N-linked glycans are generally released enzymatically and chemically producing an aldehyde reducing end.

II. OLIGOSACCHARIDE FRAGMENTATION

A. Fragmentation Nomenclature

The fragmentation of oligosaccharide ions is assigned according to the nomenclature introduced by Domon and Costello (1988) (Scheme 1) based on the peptide fragmentation, where the reducing end is positioned at the same location as the C-terminus on peptides. Product ions containing the reducing end of an oligosaccharide are designated as X (cross-ring cleavage), and Y and Z (glycosidic bond cleavage). Those fragments containing the non-reducing end are termed A (cross-ring cleavage), and B and C (glycosidic bond cleavage). Subscript numerals indicate cleavage along the glycosidic bond, whereas superscript numerals denote the position of the cross-ring cleavage (Scheme 1). Although the product ion may correspond to several possible cleavages, often only one is designated for simplicity. Because rigorous mechanistic analysis cannot be performed except in very

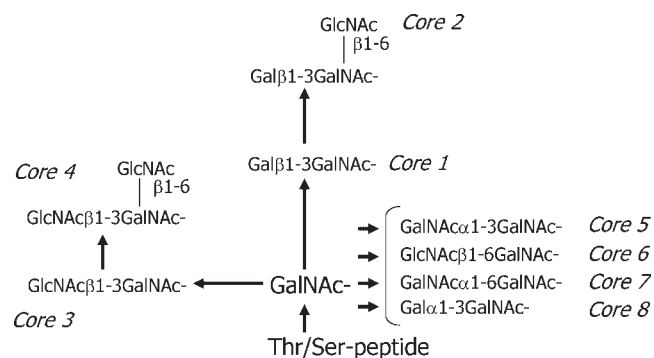


FIGURE 1. Biosynthesis pathways and currently known core-type structures of O-linked glycans.

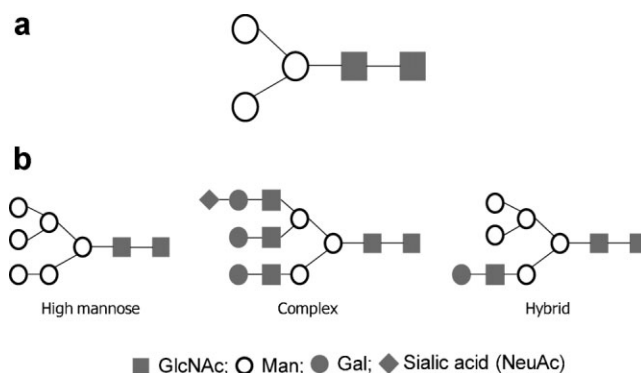


FIGURE 2. a: Trimannosyl pentasaccharide core and (b) three groups of N-linked glycan structure.

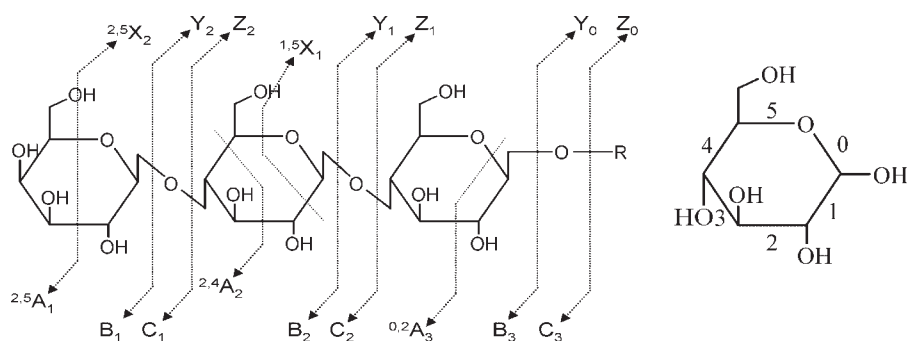
rare situations, it is always assumed that fragmentation assignments are typically proposed mechanistically and not confirmed.

B. Glycosidic Bond and Cross-Ring Cleavages

Oligosaccharides undergo two main types of fragmentation (Domon & Costello, 1988; Cancilla et al., 1999). *Glycosidic bond cleavage* occurs between two adjacent sugar rings and provides information regarding sequence and branching. *Cross-ring cleavage* involves the breaking of any two bonds on a sugar ring and is often less prevalent than glycosidic bond cleavages. They provide valuable information regarding linkages and branching. Cross-ring cleavages are not common in low-energy methods where glycosidic bond cleavage ions are the dominant products but are often observed in high-energy methods. Moreover, factors such as charge carrier (i.e., H^+ , Na^+ , etc.), the charge state, the glycans type (O-linked glycan vs. N-linked glycan), the reaction energetics, and the lifetime of the ion prior to detection can all affect the degree of oligosaccharide fragmentation and the ratio of glycosidic versus cross-ring cleavages.

The mechanisms for cross-ring cleavages and glycosidic bond cleavages have been studied but not as extensively as peptide cleavages. The most common mechanism for both cleavages of sodium co-ordinated oligosaccharide in the positive mode is depicted in Scheme 2. For glycosidic bond cleavage (Scheme 2a), the most commonly observed products are consistent with this mechanism to yield an oxonium ion intermediate. Indeed, the B-type ions are the most commonly observed fragments in the positive mode. However, this mechanism while useful and consistent with observations may not be correct. Extensive mechanistic studies by Leary and co-workers (Hofmeister, Zhou, & Leary, 1991) involving labeled precursors indicate that the most viable mechanism is that shown in Scheme 2b. Instead of oxonium ions, the intermediate involves an energetic epoxide species.

Cross-ring cleavages have not been as extensively studied mechanistically possibly due to the difficulty in producing site-specific isotopically enriched saccharides. The commonly proposed process involves a series of retro-aldol reactions to yield losses of 60, 90, and 120 mass units (Scheme 3). The products formed can be used to determine the linkages. For example, the loss of only 60 units indicates the presence of a 1,4-linkage, the loss of 90 units for 1,3-linkage, and 120 units



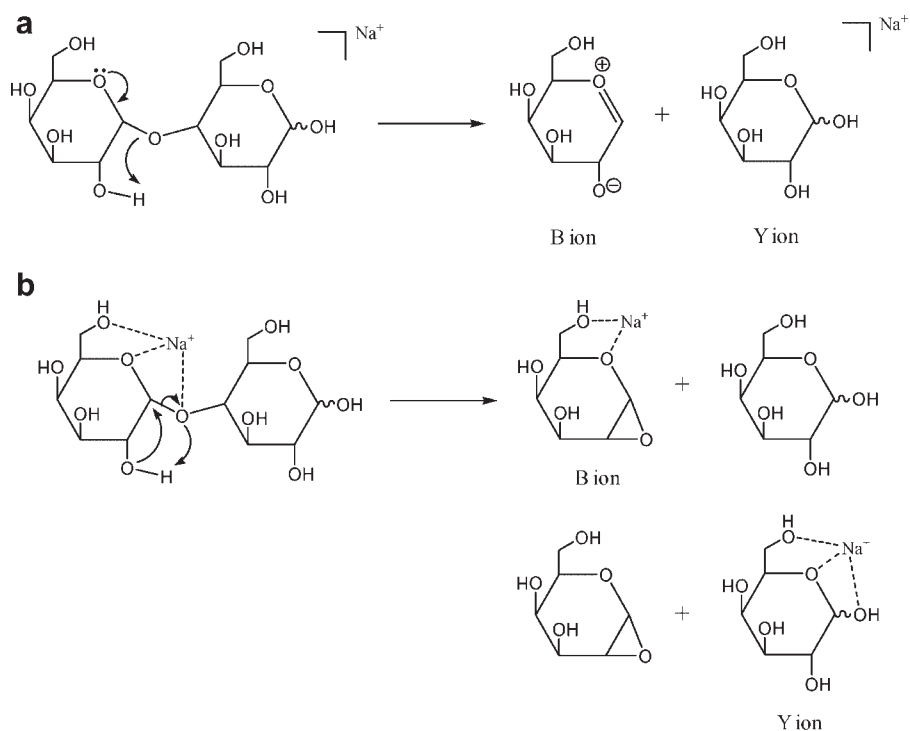
SCHEME 1. Oligosaccharide fragmentation nomenclature.

for 1,2-linkage. The losses of 60, 90, and 120 indicate 1,6-linkages (Cancilla, Penn, & Lebrilla, 1998). Unfortunately, cross-ring cleavages do not occur often enough to provide linkage information. They appear to happen less or not at all if the reducing end is reduced. Hence with O-linked glycans that are typically released with alkaline sodium borohydrate yielding the reduced oligosaccharide alditols, cross-ring cleavages are rarely observed under standard low-energy CID conditions.

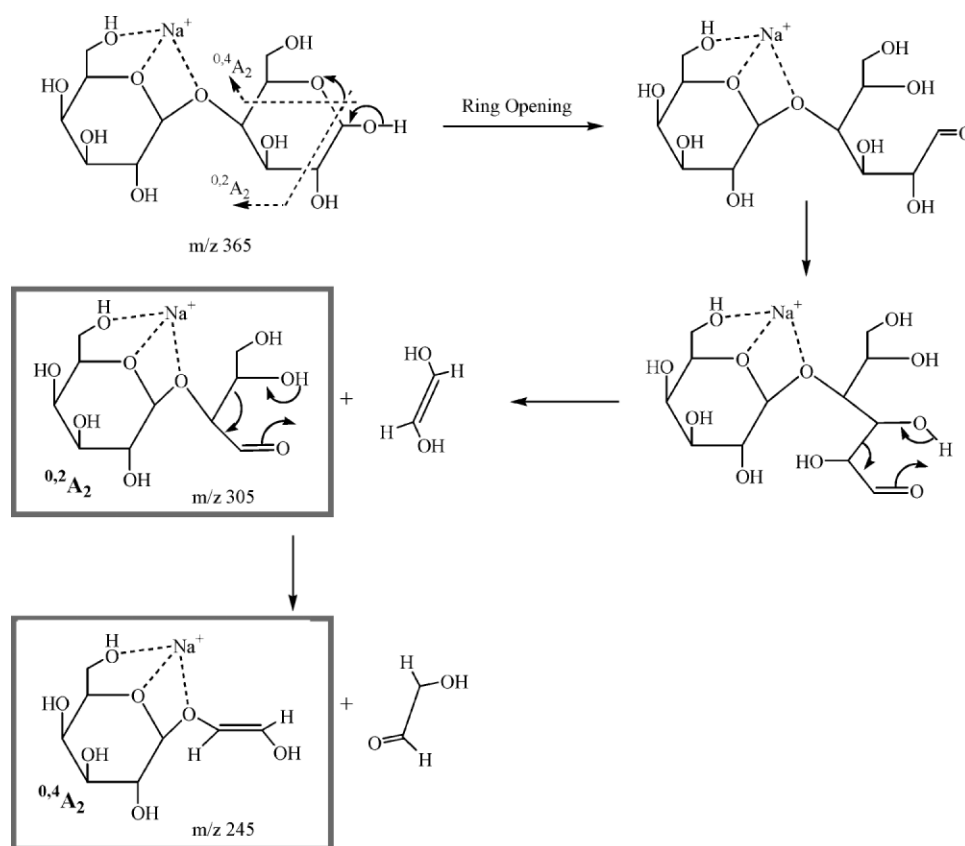
C. Internal Residue Loss

While the majority of the fragments originates from the terminal positions, rearrangement reactions cause apparent loss of residues from within. Such migration reactions obviously complicate structural elucidations. These reactions differ from the internal

fragments involving the loss of two or more sugar residues from both termini. They have been generally observed in the CID of protonated oligosaccharides derivatized with basic residues but have not been reported for sodium co-ordinated ions (Kovacik et al., 1995; Ernst, Muller, & Richter, 1997; Ma et al., 2000; Franz & Lebrilla, 2002; Harvey et al., 2002). A common occurrence is the migration of a terminal fucose resulting in the loss of an internal residue as shown by Kovacik et al. (1995), Harvey et al. (2002), and Franz and Lebrilla (2002) for fucosylated oligosaccharides. The mechanisms and molecular modeling calculations indicate the involvement of the protonated amino nitrogen atom of the derivative, which is supported by the fragment ions observed. We advise therefore to use tandem MS spectra of protonated oligosaccharides with caution as the fragmentation pattern may not be necessarily be consistent with the structure.



SCHEME 2. Proposed mechanism for glycosidic bond formation (B/Y ion) in sodium co-ordinated disaccharides in the positive mode. Two mechanisms involve the (a) oxonium ion and (b) epoxide as an intermediate, respectively.



SCHEME 3. Reaction mechanism for cross-ring cleavages of sodium coordinated disaccharides in the positive mode.

D. The Special Cases of Fucosylated and Sialylated Oligosaccharides

Fucose and sialic acid residues are structurally distinct but yield similarly labile characteristics under CID conditions. Both residues readily dissociate to lose structural information, particularly in the positive mode. Shown in Figure 3a is the CID of a sialic acid-containing compound in the positive mode. Note the major peak corresponding to the loss of sialic acid. Sialic acids are so highly labile that even during ionization, particularly with MALDI, sialic acid losses often occur unless the molecules are chemically stabilized. When the acid is esterified, then its dissociation characteristics do not differ significantly from neutral oligosaccharide residues. While there has been no mechanistic study on the dissociation of sialic acid, the fragmentation is consistent with the assistance of the acidic proton to induce fragmentation as shown in Scheme 4a. The migration of the proton to the glycosidic bond is facilitated by the relative proximity of the carboxylic acid. Converting the carboxylic acid to the ester removes the proton and stabilizes the residue (Scheme 4b). Indeed, methylating the sialic acids significantly diminishes loss of sialic acid during ionization events (Powell & Harvey, 1996; An & Lebrilla, 2001) and is a useful method for obtaining strong sialylated oligosaccharide signals in the positive mode.

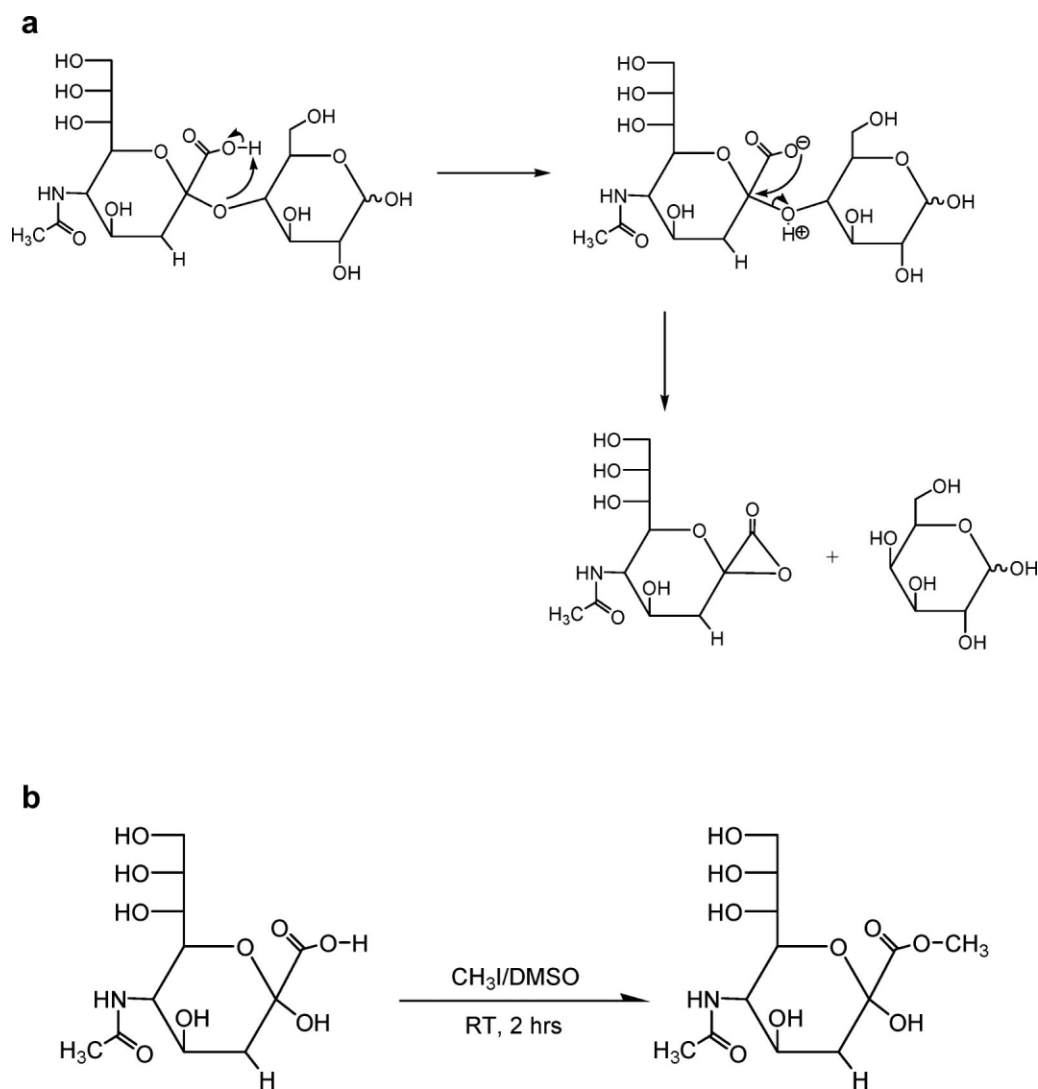
The labile nature of fucoses is more surprising given that it is a neutral oligosaccharide. The CID spectrum of a fucosylated oligosaccharide is shown in Figure 3b. The loss of fucose is one of

the first ions produced and is often produced even during ionization. There are no simple methods for stabilizing fucose residues in oligosaccharides as they are with sialic acids. Fucose differs most significantly from other neutral residues by the loss of the hydroxyl group on carbon 6. One can surmise therefore that position 6 plays a strong role in stabilizing saccharides in the terminal position, suggesting important interactions between the C_6 hydroxyl group and the other hydroxyl groups on the internal residues.

III. OLIGOSACCHARIDE FRAGMENTATION USING CID

A. Collision-Induced Dissociation (CID)

CID, also known as collision-activated dissociation (CAD), is the most commonly used method for fragmenting oligosaccharide ions. Ions collide with small neutral molecules to convert the ions' kinetic energy to vibrational energy. CID has been widely employed for structural elucidation of other biomolecules, specifically peptides. For oligosaccharides, CID can provide sequence, connectivity (branching), and even linkage and stereochemistry (Tseng, Hedrick, & Lebrilla, 1999; Dell & Morris, 2001; Harvey, 2001). This process involves first isolating the ion of interest, the precursor ion, from a mixture of ions generated during the ionization event. The ion is translationally excited and collided with an inert gas such as He, N_2 , or Ar to produce fragments. Kinetic energy from the collision is



SCHEME 4. a: Glycosidic bond cleavage of sialylated oligosaccharide and (b) esterification of sialylated oligosaccharide.

(FTICR), and hybrid quadrupole/time-of-flight (qTOF) analyzers. In the translational energy range of 1–100 eV, the resulting vibrational excitation produces a relatively narrow internal energy distribution resulting in primarily glycosidic bond cleavages. The extent of the fragmentation from a few residue losses to the production of mainly di- and trisaccharides can be controlled by increasing the translational energy and the number of collisions. The target mass has a strong influence on the tandem mass spectrum for low-energy CID (Wysocki, Kenttamaa, & Cooks, 1987). Larger target molecules such as argon and xenon can be used to increase the resulting internal energy and the extent of fragmentation at a higher cost of the gas. A simpler approach is to increase the pressure of the number of collisions and the translational energy, but these conditions can decrease sensitivity due to increased ion loss from scattering. Increasing the internal energy, by heating the collision gas particularly in ion traps, can also be effective for increasing the internal energies of the precursor ions (Wysocki, Kenttamaa, & Cooks, 1987).

In high-energy CID, the precursor ion is accelerated to kinetic energy of approximately 1 kV or higher (1–10 keV),

resulting in the excitation of electronic states in the precursor ion. Many more types of fragmentation reactions can occur because high-energy collisions produce a broad internal energy distribution. In addition, because ion scattering can be a major problem, there is a narrow parameter window where MS^n spectra can be obtained. Therefore, high-energy CID spectra often have the appearance of being more reproducible than low-energy CID.

Previously, high-energy CID experiments were performed with sector-based tandem mass spectrometers using fast atom bombardment (FAB) or liquid secondary ion MS (LSIMS) ionization (Harvey, Bateman, & Green, 1997). However, these instruments are becoming less common owing to the significantly poorer sensitivity of FAB and LSIMS. More recently, MALDI-TOF/TOF has been shown to produce high-energy collision conditions for oligosaccharides. These instruments have significantly higher sensitivities for oligosaccharides compared to the earlier generation of sector-based tandem mass spectrometers using FAB or LSIMS ionization. In TOF/TOF, high-velocity ions produced in a high vacuum pulsed MALDI-TOF are selected with a timed ion gate to yield keV energy for collisions. The ions

are further accelerated in a two-stage reflectron TOF. High-energy collision conditions produce larger fractions of cross-ring cleavages such as A- and X-type ions (Mechref, Novotny, & Krishnan, 2003; Stephens et al., 2004). While the information is crucial for elucidating the structure of oligosaccharides, high-energy CID often yields many peaks that are artifacts due to metastable dissociation. Interpreting the spectra of unknown compounds is therefore complicated by the presence of spurious peaks.

B. Low-Energy CID Experiments

Low-energy CID spectra are significantly less complicated than high-energy CID. These experiments are performed in instruments such as multiple-quadrupole (e.g., triple quadrupole MS), linear, and 3-D ion traps, and FTICR instruments. In these techniques, CID can be performed either in-time or in-space. Multiple quadrupole instruments such as triple quadrupoles select ions with a first set of quadrupole, perform CID within the second quadrupole, and measure the products with the third quadrupole. Ion traps and Fourier transform instruments employ in-time isolation. These methods destabilize the trajectory of all other ions except for the ion of interest. Since the results presented below were obtained on an FTICR, CID on these instruments will be discussed in greater detail. However, our experiences with quadrupole ion traps indicate that the fragment ion products are the same.

In the ion cyclotron resonance (ICR) cell, the selected ions are translationally excited by two modes. The first is on-resonance excitation where the ion is translationally excited at a frequency equal to the ions' cyclotron frequency (Cody & Freiser, 1982; Cody, Burnier, & Freiser, 1982; Cody et al., 1982). The event can increase the translation energy to approximately 100 eV, depending on the size of the magnet. In this method, the ions are translationally excited to a larger cyclotron orbit. The precursor ions can also be excited in a periodic fashion by the application of a sustained off-resonance irradiation (SORI) pulse (typically ≥ 600 msec) of alternating electric field pulse with a frequency slightly lower (or higher) than the ions' natural cyclotron resonance frequency (RF) (Gauthier, Trautman, & Jacobson, 1991). A constant RF level is applied to the excite electrodes throughout the CID event. As a consequence, the ions undergo acceleration–deceleration cycles and thus a sequential activation of ions by multiple collisions of low translational energy (< 10 eV) with target gas throughout the duration of the electric field pulse. Spatially, the ions experience the correspond-

ing cycles of being excited to a small radius away from the ICR cell center, then relaxing back to the center. The precursor and fragment ions hover near the center of the cell allowing additional stages of CID and stronger intensities during detection. SORI-CID can facilitate the lowest energy pathway of fragmentation of precursor ions as only small increments of internal energy are deposited in the ions throughout the duration of the event. SORI has been the main mode of CID used for oligosaccharide fragmentation (Tseng, Hedrick, & Lebrilla, 1999; Mirgorodskaya, O'Connor, & Costello, 2002).

C. Interpretation of CID MS Spectra

Determination of oligosaccharide composition is simplified by high mass accuracy and resolution; however, interpretation of tandem MS spectra is sufficient with most unit-mass resolution instruments. Table 1 lists the monoisotopic and residue masses of common mammalian monosaccharide. A good understanding of glycobiology is also extremely useful. There are significant heterogeneity and structural diversity in oligosaccharides; however, naturally occurring oligosaccharides are synthesized with a finite set of glycosyl transferases along essentially conserved pathways. Therefore, the possibilities of monosaccharide combinations may seem infinite, yet biology severely limits this number to a manageable pool.

Shown in Figure 1 are the eight known core structures of O-linked glycans (Brockhausen, 1999). The O-linked glycans are more amenable to CID because of their smaller size, thus, they will be used as the CID examples. Examples of N-linked glycans will be given below using IRMPD. The interpretation of tandem MS spectra of an O-linked glycan produced by MALDI and coordinated to sodium (Na^+) is illustrated with Figure 4. The compound was released from mucins and reduced to yield the alditol. O-linked glycans are typically released by alkaline sodium borohydrate to yield the resulting reducing end alditol. Oligosaccharide composition of the compound is readily determined initially from the accurate mass determined by FTICR MS. The molecular ion m/z 1268.473 ($[\text{M} + \text{Na}]^+$) corresponds to two hexoses (Hex), two fucoses (Fuc), and three *N*-acetylhexosamines (HexNAc) (theoretical mass 1268.475, $\Delta m = 0.002$ Da). The composition is readily confirmed by the CID spectrum as shown. The quasimolecular ion yields the losses in sequence of one fucose (m/z 1,122) and the loss of second fucoses (m/z 976). The losses of a hexose (m/z 1,106) as well as a HexNAc (m/z 1,065) from the quasimolecular ion show the presence of both on the non-reducing end. This spectrum also

TABLE 1. Monoisotopic and residue mass for common monosaccharide found in mammalian glycosylation

| Monosaccharide | Abbreviation | Monoisotopic mass | Monoisotopic residue mass (-H ₂ O) |
|---|--------------|-------------------|---|
| Fucose | Fuc | 164.0685 | 146.0579 |
| Hexose ^a | Hex | 180.0634 | 162.0528 |
| <i>N</i> -acetylhexosamine ^b | HexNAc | 221.0899 | 203.0794 |
| <i>N</i> -acetyl neuraminic acid | NeuAc | 309.1060 | 291.0954 |
| <i>N</i> -glycolyl neuraminic acid | NeuGc | 325.1008 | 307.0903 |

^aHexose contains glucose (Glc), galactose (Gal), and mannose (Man).

^b*N*-acetylhexosamine contains *N*-acetylglucosamine (GlcNAc) and *N*-acetylgalactosamine (GalNAc).

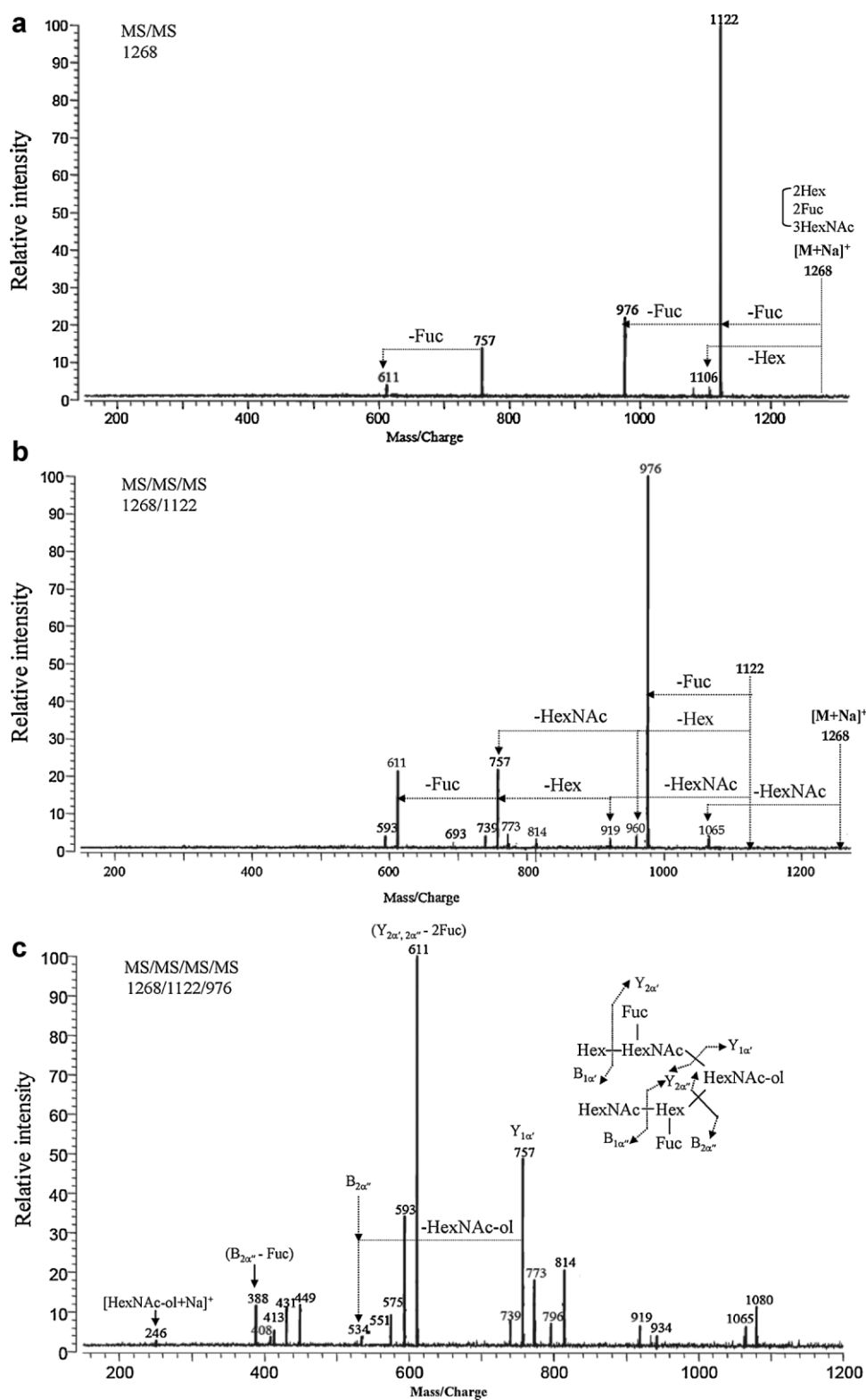
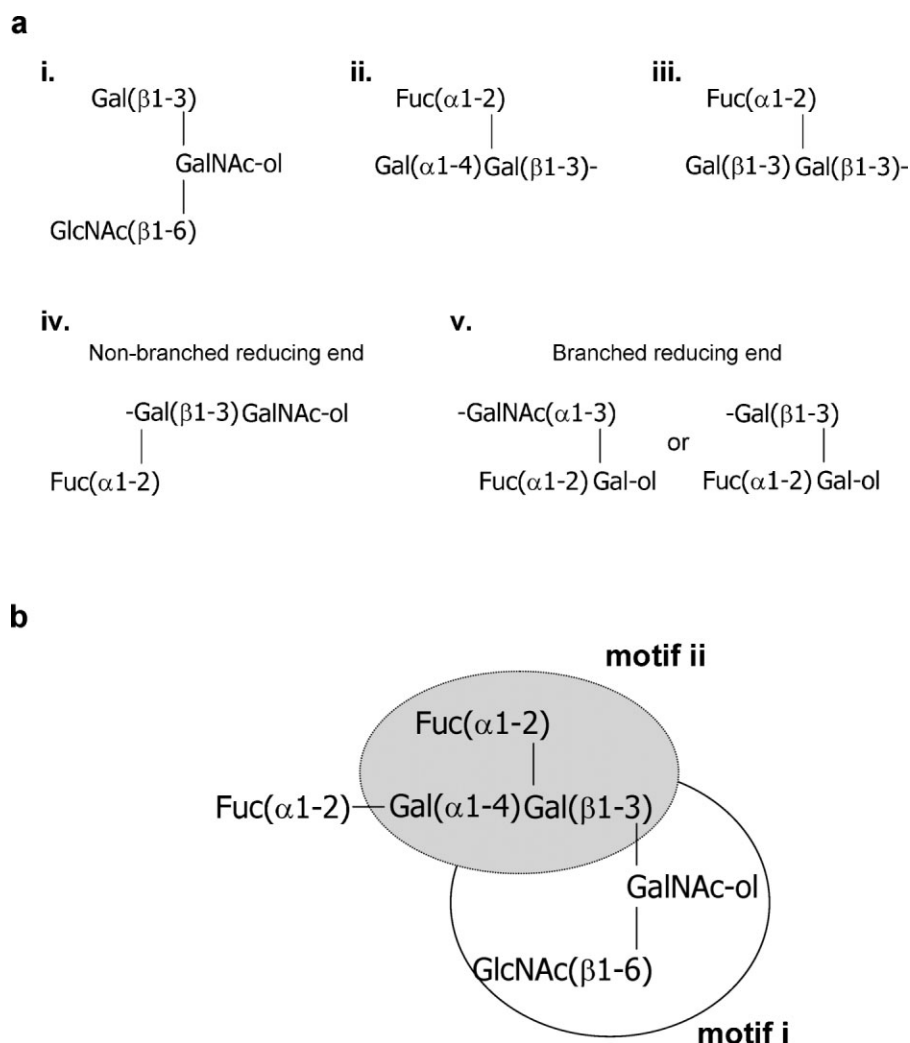


FIGURE 4. MALDI-CID tandem mass spectra of O-linked glycans (m/z 1,268) from egg jelly glycoprotein of *Xenopus tropicalis* in the positive mode. **a:** MS² spectrum of the precursor ion, **(b)** MS³ (1,268 → 1,122) spectrum, and **(c)** MS⁴ (1,268 → 1,122 → 976) spectrum.



SCHEME 5. **a:** Five structural motifs identified by mass spectrometry from the 12 known structures of neutral oligosaccharides found in the jelly coats of the eggs of *Xenopus laevis*. **b:** Example of an oligosaccharide with two substructural motifs found in the catalog.

(Hex) and a fucose (m/z 757 and 773, respectively). Both ionic species in turn lose a Fuc and a Hex, respectively, to produce a single product at m/z 611. The fragmentation pattern is easily recognizable and corresponds to motif ii (Scheme 5). To obtain the structural motifs corresponding to the remainder of the molecule, an MS^4 experiment was performed by following the sequence m/z 1,065 \rightarrow 919 \rightarrow 773. Motif i was characterized by the presence of several peaks including m/z 390, 408, 431, 449, and 413. The structures based on these motifs are presented (Fig. 6b, inset).

IV. OLIGOSACCHARIDE FRAGMENTATION USING IRMPD

A. Infrared Multiphoton Dissociation (IRMPD)

Vibrational excitation and dissociation using IRMPD has been used to study the chemistry of small molecules for decades (Baer & Brauman, 1992; Marzluff et al., 1994). More recently, IRMPD is used for the structural characterization of intact proteins (Tsybin et al., 2004; Jebanathirajah et al., 2005), peptides

(Kosaka et al., 2003; Wilson & Brodbelt, 2006), oligonucleotides (Little et al., 1996; Hofstadler et al., 1998; Hakansson et al., 2003; Gabelica et al., 2008), and oligosaccharides (Zhang et al., 2005; Lancaster et al., 2006; Pikulski et al., 2007).

IRMPD is a dissociation technique that yields very similar fragments to CID. The resonant absorption of a few IR photons with relatively low energy allows the ions of interest to fragment selectively along its lowest energy dissociation pathways. Typically, IRMPD employs photons supplied by a 10.6 μm CO_2 laser. Tunable laser has recently been used to obtain specific fragments (Watson et al., 1991; Peiris, Riveros, & Eyler, 1996).

IRMPD is especially well suited for the dissociation of trapped ions in an FTICR cell. A typical pulse sequence for IRMPD in MALDI-FTICR MS was shown in Figure 7. The Nd:YAG laser was fired five times at 1,000 msec intervals to produce ions for transport into the ICR cell. A desired ion is selected in the analyzer with the use of an arbitrary waveform generator and a frequency synthesizer. The CO_2 infrared laser was fired at 8,000 msec with the width 200–1,500 msec, depending on the molecular size and structure of the target ion, while the trapping plates were elevated to +4 V. The voltages on

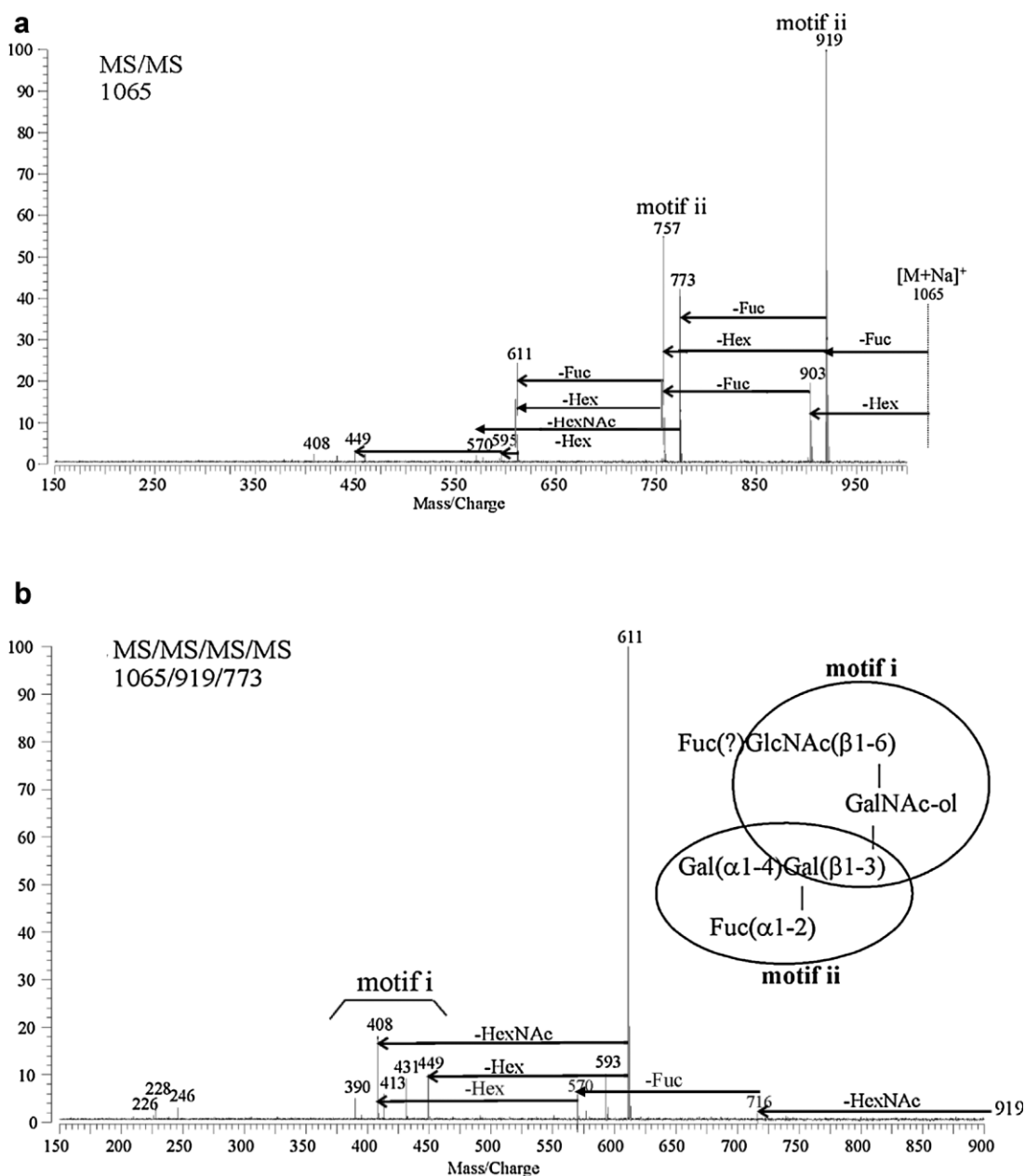


FIGURE 6. CID mass spectra of neutral oligosaccharide, m/z 1,065. **a:** MS^2 CID spectrum and **(b)** MS^4 CID spectrum (m/z 1,065 \rightarrow 919 \rightarrow 773).

the trapping plates were then ramped down to +1.2 V from 15,000 to 16,000 msec for detection. The laser is typically focused at the center of the ICR cells.

IRMPD offers a number of advantages for biomolecule sequencing. The main advantage of IRMPD over CID is that no collision gas is needed for dissociation of precursor ions. Consequently, there is no degradation of the high vacuum during the analysis. In addition, analysis can be performed much faster because there is no pump-down delay (Li et al., 1999). Moreover, IR photon absorption does not cause translational excitation of ions as does CID, thereby minimizing ion losses due to ejection or ion scattering. As both the precursor and product ions absorb IR photons, more extensive fragmentation but still structurally relevant fragments are obtained. IRMPD therefore provides on-

axis fragmentation yielding more product ions and better control of excitation energy with minimal mass discrimination.

B. Dependence of IRMPD Fragments on Increasing Oligosaccharide Size

CID is notoriously inefficient in fragmenting large ions. The fragmentation efficiencies of large molecules are limited by both the decrease in the center of mass collision energy, associated with the increasing precursor ion mass, and the dimension of the ICR cell (Williams, Furlong, & McLafferty, 1990). Furthermore, when the parent ions are translationally excited, the product ions may diffuse radially due to magnetron orbit expansion (Francl, Fukuda, & Mciver, 1983). Larger ions commonly require

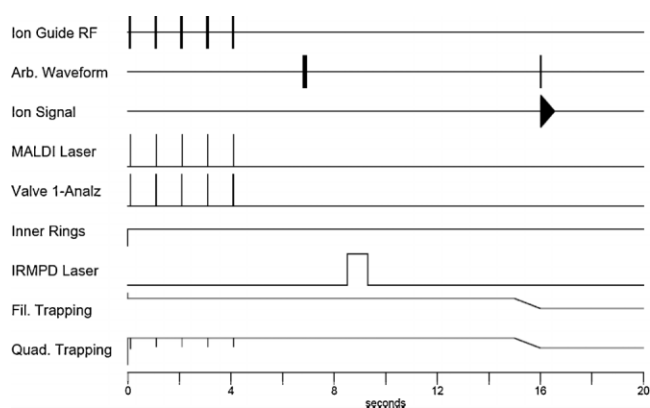


FIGURE 7. A typical pulse sequence for IRMPD in MALDI-FTICR.

multiple CID events (MS^n , $n > 2$) for complete fragmentation and structural determination. Each isolation/fragmentation event causes ion loss, and a decrease in signal is inevitable. In our experience, CID works well for ions below m/z 1,500 but becomes more difficult for oligosaccharides ions above m/z 1,500. On the contrary, IRMPD works well for ions with m/z above 500 and increases in fragmentation efficiency as the ions increase beyond m/z 2,000 (Xie & Lebrilla, 2003; Zhang et al., 2005; Lancaster et al., 2006). In our laboratory a systematic study was performed to determine whether the IRMPD efficiency correlated with the sizes of oligosaccharides (Zhang et al., 2005). IRMPD with the same irradiation period and constant laser power was achieved to obtain the fragments from five different oligosaccharide sizes consisting of tri-, penta-, hexa-, hepta-, and octasaccharide having the same core structure (Gal:GalNAc:GalNAc-ol). The quasimolecular ion of the octasaccharide was dissociated completely under the given condition while only 10% of the trisaccharide was decomposed. The fragmentation dramatically increased with increasing size. IRMPD is therefore suitable for small molecules, medium-sized molecules, and larger macromolecules, but it works best on medium-sized and larger molecules. These results suggest that the high fragmentation efficiency of high mass ions may attribute to the rapid increase of the density of vibrational states with increasing molecular sizes.

C. Interpretation of IRMPD Spectra for O-Linked Glycans

The IRMPD spectrum of an O-linked oligosaccharide (m/z 1065.396, $[M + Na]^+$) is shown in Figure 8. The oligosaccharide composition corresponding to two Hex, two Fuc, and two HexNAc was determined based on the exact masses obtained from FTICR MS. The primary sequence and branching of oligosaccharide was elucidated by IRMPD.

The ions ranging from the precursor ion to the terminal monosaccharide residue (m/z 228) corresponding to $[HexNAc-ol-H_2O + Na]^+$ were readily obtained in a single tandem mass event. Loss of two consecutive fucoses from the quasimolecular ion (m/z 1,065 \rightarrow 919 \rightarrow 773) as major fragment ions was observed, indicating that two Fuc residues were non-reducing terminal positions with at least one branched point. There is no direct Hex loss from the quasimolecular ion, suggesting that the two Hex are internal. It is noted that the loss of HexNAc (m/z 570)

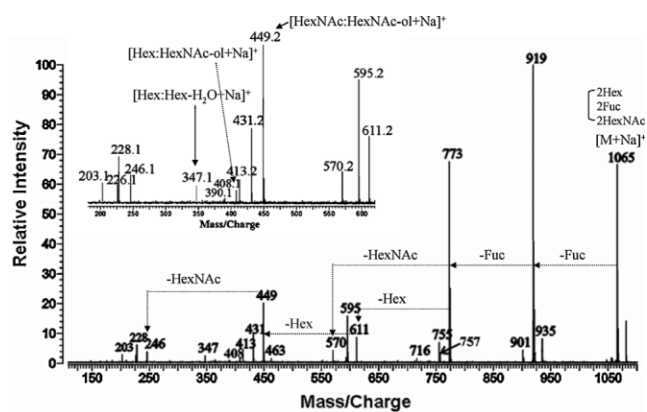
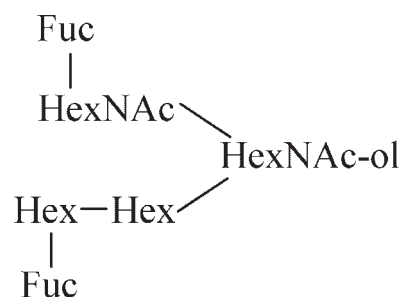


FIGURE 8. IRMPD mass spectrum of m/z 1,065 in MALDI-FTICR MS. All representative fragment ions present in the multistage CID spectra (Fig. 6) are observed in the IRMPD spectra.

and the loss of Hex (m/z 611) from the same precursor ion m/z 773 occurs by two separate pathways: (1) the former follows the loss of one HexNAc on terminal position because there is no further loss and (2) the latter presents the loss of the internal Hex. The ion at m/z 611 corresponding to one Hex, one HexNAc, and HexNAc-ol identify the presence of the known trisaccharide core, which is also the most common core structure for mucin-type oligosaccharides. It can further lose one Hex and HexNAc (m/z 611 \rightarrow 449 \rightarrow 246) consecutively or vice versa (m/z 611 \rightarrow 408 \rightarrow 246). The presence of two peaks at m/z 408 and 449 corresponding to $[Hex-HexNAc-ol + Na]^+$ and $[HexNAc-HexNAc-ol + Na]^+$, respectively, indicates that both Hex and HexNAc are bound to HexNAc-ol. The presence of m/z 347 ($[Hex:Hex-H_2O + Na]^+$) ion confirmed the assignments that two Hex are connected each other as an internal. Therefore, the primary sequence of the ion m/z 1,065 could be determined as follows:



D. Interpretation of IRMPD Spectra for N-Linked Glycans

IRMPD is an ideal technique for fragmenting large oligosaccharides especially for N-linked glycans, which are relatively large compounds that are not readily fragmented with low-energy CID techniques. The structures of N-linked glycans significantly differ from O-linked glycans so that they require their own investigation. N-linked glycans (Fig. 2) containing a highly branched core structure have high masses and require multiple isolation/fragmentation events for complete structural elucidation. This feature makes complete structural determination of N-linked glycans with CID difficult.

For N-linked glycans, the goals of tandem MS are to confirm the putative structure deduced from known glycobiology and to obtain linkage information through cross-ring cleavages. The IRMPD spectrum of the Man₉ (m/z 1905.6, [M + Na]⁺) consisting of two GlcNAc and nine mannoses is shown in Figure 9. The putative structure can be deduced from glycan composition because all N-linked glycans share a common trimannosyl core structure consisting of mannose and GalNAc residues (Man₃GalNAc₂). The extensive fragmentation was observed in a single MS/MS event. An oligosaccharide with quasimolecular ion at m/z 1905.634 has two possible compositions within 10 ppm mass tolerance. Only one composition consisting of nine Hex and two HexNAc can be correctly assigned as a N-linked glycan (Fig. 2).

The glycosidic bond cleavages (Fig. 9b), B₅, and B₄ ions (m/z 1,685 and 1,481, respectively) were readily observed along with fragments corresponding to subsequent mannose losses (i.e., m/z 1,685, 1,523, 1,361, 1,199, 1,037, 875, 712 and m/z 1,481, 1,319, 1,157, 995, 833, 671, 509). The ion at m/z 509 corresponds to the trimannosyl core ([Man₃-H₂O + Na]⁺). Furthermore, C₄ fragments (m/z 1,499) and subsequent losses of mannose (C₄/Y_{*n*}) were clearly shown. These ions were present at m/z 1,337, 1,175, 1,013, 851, 689, and 527. Some internal fragments were also present in the IRMPD spectrum. These fragments corresponded to products of cross-ring cleavages occurring at the core branching mannose (Fig. 9c). These ions were present at m/z 893, 731, and 569 and corresponded to the ^{0,4}A₄ ion with subsequent double mannose losses, respectively. Another series of cross-ring cleavages representing the ^{0,3}A₄ fragment from the same mannose core with subsequent mannose losses (m/z 923, 761, and 599) were observed and were more intense than the ^{0,4}A₄ series. A minor fragment corresponding to ^{0,4}A₄/Y_{5α'} was also observed (m/z 731) with an accompanying mannose loss (^{0,4}A₄/Y_{5α}, m/z 569). A fragment ion, ^{0,2}A₆, corresponding to the cross-ring cleavage of the reducing end, was the largest fragment ion detected (m/z 1,806). The cross-ring cleavages were limited, but provided information regarding the first branched residue and the linkages of the antennae. The fragmentation patterns observed in the IRMPD spectrum provided substantial information for structural elucidation of GlcNAc₂Man₉.

Complex type N-linked glycans including sialic acids with labile moieties were also examined (Lancaster et al., 2006). The IRMPD spectrum of monosialylated triantennary N-linked glycan obtained from bovine fetuin is shown in Figure 10. The putative glycan structure (inset in Fig. 10) could be deduced from known glycobiology and glycan composition obtained from accurate mass. The sodiated parent ion, m/z 2,341 [M-H + 2Na]⁺ consisting of 3Hex:3HexNAc:1NeuAc with a trimannosyl core (Man₃GlcNAc₂), was readily dissociated due to the facile loss of sialic acid (-[NeuAc-H + Na]) to yield the Y₆ ion (m/z 2,027). This fragment ion further dissociated to produce essentially all other fragment ions such as glycosidic bond (Fig. 10b) and cross-ring cleavages (Fig. 10c). No fragment ions containing a sialic acid were observed. Subsequent losses consisting of the combinations of reducing and non-reducing end fragments helped to elucidate the structure. For clarity, the combinations of losses are designated by “/” and include several series such as B_{*n*} and Y_{*n*}. For example, the B₆/Y₆ fragments come from the loss of the sialic acid and the GlcNAc core (m/z 2,341 → 2,027 → 1,806). Other ions due to combination of cleavages include B₆/Y_{6,5α'} (m/z 1,644), B₆/Y_{6,4α'} (m/z 1,441),

B₆/Y_{6,4α',5α''} (m/z 1,279), and B₆/Y_{6,4α',4α''} (m/z 1,076). These losses help define the connectivity of the glycan shown in Figure 10. A number of cross-ring cleavages at the reducing end and branch points were observed. These include ^{0,2}A₇/Y₆, ^{0,2}A₅/Y₆, ^{2,4}A₇/Y₆, and ^{2,4}A₆/Y₆.

The fragmentation observed in the IRMPD spectra of N-linked glycans yielded primarily glycosidic bond cleavages with cross-ring cleavages at the core branching mannose and reducing end.

E. Diagnostic Fragment Ions of N- and O-Linked Glycans

While there is great diversity in glycan structures, there are also many similarities that translate to common signals indicative of specific structural features. For example, the core structures of the N-linked glycans yield a number of diagnostic signals that are readily interpreted in the tandem MS. Shown in Table 2 are the most commonly observed signals in tandem MS of N- and O-linked glycans.

The common core of N-linked glycan consists of two GlcNAc and three mannoses (Man). The tandem MS of N-linked glycans often include the trimannosyl group (Table 2) with ion at m/z 509 corresponding to [3Man-H₂O + Na]⁺. Signals at m/z 712 and 874 are also commonly observed fragments with all N-linked glycan, while the m/z 915 and 1,077 are observed only with complex and hybrid-type glycans. N-linked glycans also often yield cross-ring cleavages at the reducing end. The ions at m/z 772, 975, and 1,137 represent the most common cross-ring cleavage (^{2,4}A) occurring at the reducing end GlcNAc.

O-linked glycans have several core structures and have fewer MS signals in common. A common signal for all however include m/z 246 corresponding to the reduced GalNAc and is unique only to reduced O-linked glycan. The ions with m/z 408 and 449 and 611 are also unique to O-linked glycans and represent core 1 and 2 structures, respectively (Brockhausen, 1999). The ions with at m/z 347, 388, and 429 are also commonly observed corresponding to internal fragments.

F. Interpretation of Tandem Mass Spectra by Computer Software

Software for automatically interpreting tandem MS spectra of oligosaccharides has been developed, most very recently. Web-based tools and databases for structural analysis of glycans were recently reviewed (Perez & Mulloy, 2005; Ceroni et al., 2008). All automated annotation software suffer the intrinsic limitations of the tandem MS, namely the lack of information regarding linkage and stereochemistry.

These approaches match peaks with corresponding *in silico* fragments of glycans. The earliest approaches were very limited. *STAT* (Gaucher, Morrow, & Leary, 2000) was used for the assignment of N-linked glycans in bacterial lipooligosaccharides. *StrOligo* (Ethier et al., 2003) was used primarily for complex oligosaccharides. *GLYCH* (Tang, Mechref, & Novotny, 2005) was based on peptide de novo sequencing programs applied to biantennary glycans.

The newer approaches combine existing databases to match structures and biological significance. Those that deal mainly with N-linked glycans include *GlycosidiQ* (Joshi et al., 2004), which uses only known glycans in its library, and

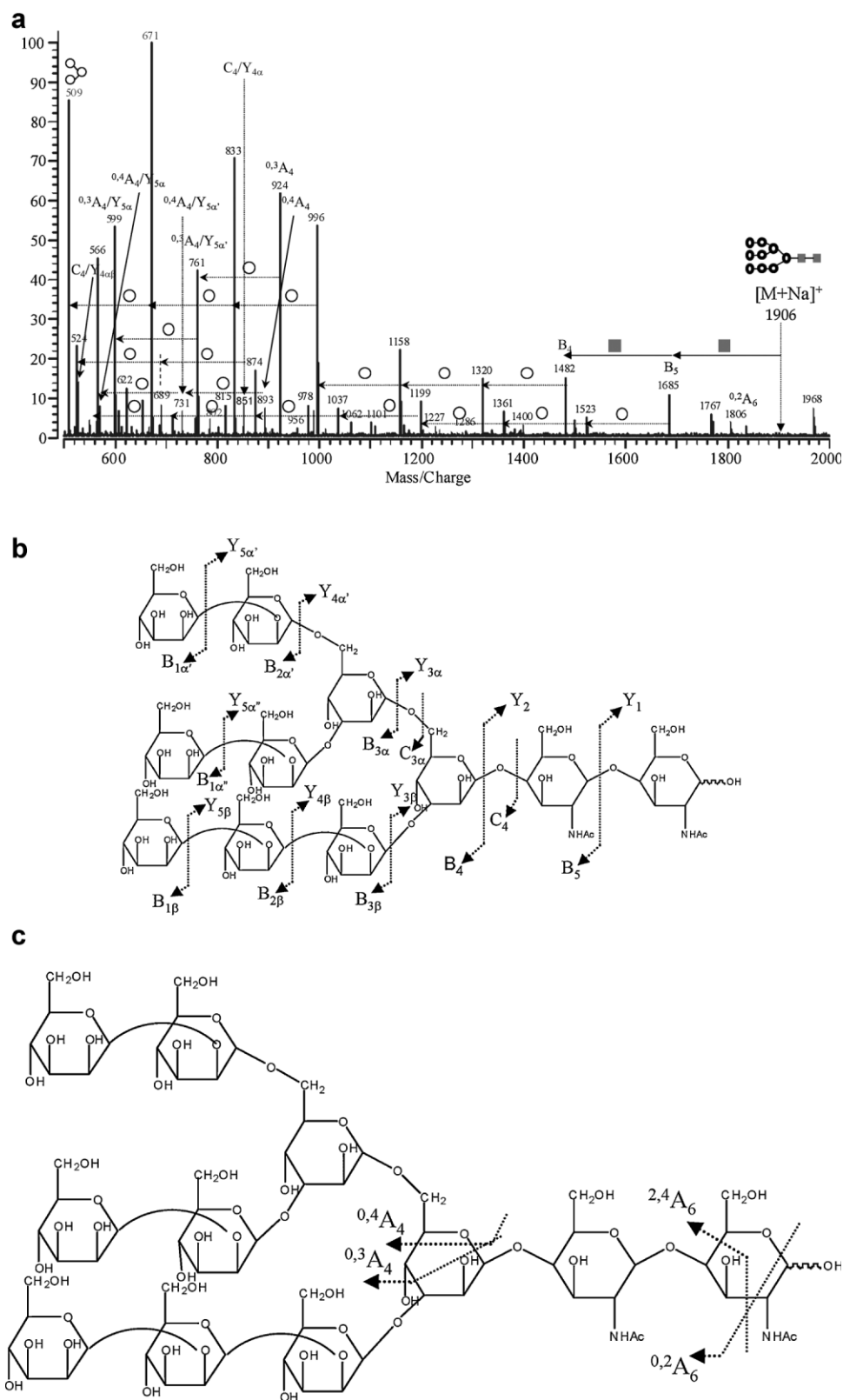


FIGURE 9. a: IRMPD spectrum of Man9 in MALDI-FT ICR MS. b: Glycosidic cleavages and (c) cross-ring cleavages found in IRMPD spectrum.

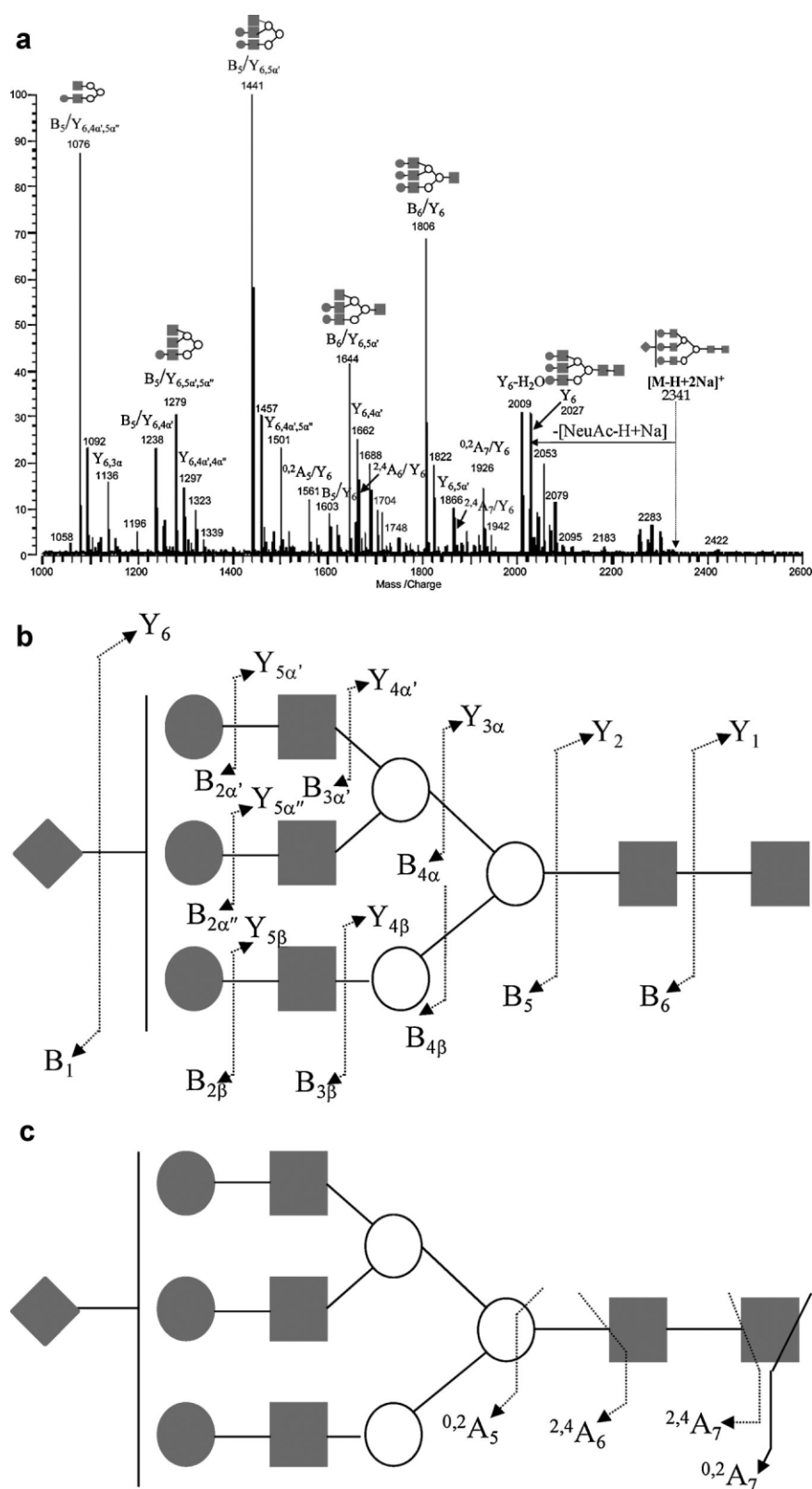


FIGURE 10. a: IRMPD spectrum of monosialylated triantennary N-linked glycan in MALDI-FT ICR MS, (b) glycosidic cleavages, and (c) cross-ring cleavages found in IRMPD spectrum.

TABLE 2. Commonly observed oligosaccharide fragments during tandem MS event

| | <i>m/z</i> | Fragment ion | Structure | Note |
|--|------------------|---|-----------|--------------------|
| O-linked glycan Reduced reducing end as an alditol | 246 | [GalNAc-ol+Na] ⁺ | | reducing end |
| | 347 | [2Hex-H ₂ O+Na] ⁺ | | internal fragment |
| | 388 | [Hex:HexNAc-H ₂ O+Na] ⁺ | | internal fragment |
| | 408 | [Hex:GalNAc-ol+Na] ⁺ | | core1 ^a |
| | 429 | [2HexNAc+Na] ⁺ | | internal fragment |
| | 449 | [HexNAc:GalNAc-ol+Na] ⁺ | | core2 ^a |
| | 611 | [Hex:HexNAc:GalNAc-ol+Na] ⁺ | | core2 ^a |
| N-linked glycan Reducing end as an aldehyde | 347 | [2Hex-H ₂ O+Na] ⁺ | | internal fragment |
| | 388 | [Hex:HexNAc-H ₂ O+Na] ⁺ | | internal fragment |
| | 509 | [3Man-H ₂ O+Na] ⁺ | | Trimannosyl core |
| | 712 | [3Man:1HexNAc-H ₂ O+Na] ⁺ | | All type |
| | 874 | [3Man:1Hex:1HexNAc-H ₂ O+Na] ⁺ | | All type |
| | 915 | [3Man:2HexNAc-H ₂ O+Na] ⁺ | | complex/hybrid |
| | 1077 | [3Man:1Hex:2HexNAc-H ₂ O+Na] ⁺ | | complex/hybrid |
| | 772 ^b | [3Man:2GlcNAc- ^{2,4} A+Na] ⁺ | | All type |
| | 975 | [3Man:1HexNAc:2GlcNAc- ^{2,4} A+Na] ⁺ | | complex/hybrid |
| | 1137 | [3Man:1HexNAc:1Hex:2GlcNAc- ^{2,4} A+Na] ⁺ | | complex/hybrid |

○, Man; ●, Hex; □, HexNAc; ■, GlcNAc; ◻, GalNAc.

^aSee Figure 1 and Reference.

^b^{2,4}A is cross-ring cleavage occurring at reducing and GlcNAc.

GlycoFragment/GlycoSearchMS (Lohmann & von der Lieth, 2004), which includes hypothetical glycan structures. *Glyco-Workbench* (Ceroni et al., 2008) was designed specifically to assist those with greater knowledge of glycan MS with annotation of glycan fragment spectra.

For completeness, a number of other softwares mainly for annotation include *GlycoMod* (Cooper, Gasteiger, & Packer, 2001), a web-based tool for compositional analysis with the derived composition searched for matching structures in the library *GlycoSuiteDB* (Cooper et al., 2001). *Glyco-Peakfinder* (Maass et al., 2007) is a more recent web-based algorithm for annotation using the EuroCarb database. A different paradigm to composition prediction was adopted in *Cartoonist* (Goldberg et al., 2005). This tool maps glycans based on a library created by incorporating the biosynthetic pathways in mammalian organism to select the most biologically feasible molecules.

One approach covers O-linked glycan. *Cartoonist Two* (Goldberg et al., 2006) is a program for interpreting tandem MS spectra of O-linked glycan. The software uses an algorithm that generates all possible cartoons of O-linked fragments consistent with the total mass and scores each accordingly.

V. CONCLUSION

The fragmentation observed in the CID (low or high energy) and IRMPD spectra yields primarily glycosidic bond cleavages with cross-ring cleavages. Oligosaccharides often yield cross-ring cleavages at the reducing end, unless the compound is reduced to the alditol. High-energy collision conditions produce larger fractions of cross-ring cleavages for both N- and O-linked glycans. However, cross-ring cleavages of internal residues under low-energy CID conditions are less common than glycosidic

bond cleavages. Cross-ring cleavages of internal residues do occur more often with N-linked glycans at the core branching mannose under both CID and IRMPD conditions.

Tandem MS is emerging as an essential technique for structural elucidation of glycans because of its intrinsic sensitivity and speed. However, complete structural elucidation is often not being possible with MS alone. The use of enzymatic reactions such as those briefly mentioned here and chemical degradation methods (Cancilla, Penn, & Lebrilla, 1998) in conjunction with tandem MS do provide a powerful tool for complete structural elucidation.

REFERENCES

- An HJ, Lebrilla CB. 2001. Suppression of sialylated by sulfated oligosaccharides in negative MALDI-FTMS. *Isr J Chem* 41:117–127.
- An HJ, Ninonuevo M, Aguilan J, Liu H, Lebrilla CB, Alvarenga LS, Mannis MJ. 2005. Glycomics analyses of tear fluid for the diagnostic detection of ocular rosacea. *J Proteome Res* 4:1981–1987.
- An HJ, Miyamoto S, Lancaster KS, Kirmiz C, Li BS, Lam KS, Leiserowitz GS, Lebrilla CB. 2006. Profiling of glycans in serum for the discovery of potential biomarkers for ovarian cancer. *J Proteome Res* 5:1626–1635.
- Apweiler R, Hermjakob H, Sharon N. 1999. On the frequency of protein glycosylation, as deduced from analysis of the SWISS-PROT database. *Biochim Biophys Acta* 1473:4–8.
- Baer S, Brauman JI. 1992. Infrared multiple photon studies of alkoxide alcohol complexes. *J Am Chem Soc* 114:5733–5741.
- Brockhausen I. 1999. Pathways of O-glycan biosynthesis in cancer cells. *Biochim Biophys Acta* 1473:67–95.
- Cancilla MT, Penn SG, Lebrilla CB. 1998. Alkaline degradation of oligosaccharides coupled with matrix-assisted laser desorption/ionization Fourier transform mass spectrometry: A method for sequencing oligosaccharides. *Anal Chem* 70:663–672.
- Cancilla MT, Wang AW, Voss LR, Lebrilla CB. 1999. Fragmentation reactions in the mass spectrometry analysis of neutral oligosaccharides. *Anal Chem* 71:3206–3218.
- Ceroni A, Maass K, Geyer H, Geyer R, Dell A, Haslam SM. 2008. GlycoWorkbench: A tool for the computer-assisted annotation of mass spectra of glycans. *J Proteome Res* 7:1650–1659.
- Chen GD, Pramanik BN. 2008. LC-MS for protein characterization: Current capabilities and future trends. *Expert Rev Proteomics* 5:435–444.
- Chi LL, Amster J, Linhardt RJ. 2005. Mass spectrometry for the analysis of highly charged sulfated carbohydrates. *Curr Anal Chem* 1:223–240.
- Cody RB, Freiser BS. 1982. Collision-induced dissociation in a Fourier-transform mass spectrometer. *Int J Mass Spectrom Ion Processes* 41:199–204.
- Cody RB, Burnier RC, Cassady CJ, Freiser BS. 1982. Consecutive collision-induced dissociations in Fourier-transform mass spectrometry. *Anal Chem* 54:2225–2228.
- Cody RB, Burnier RC, Freiser BS. 1982. Collision-induced dissociation with Fourier-transform mass spectrometry. *Anal Chem* 54:96–101.
- Cooke CL, An HJ, Kim J, Solnick JV, Lebrilla CB. 2007. Method for profiling mucin oligosaccharides from gastric biopsies of rhesus monkeys with and without *Helicobacter pylori* infection. *Anal Chem* 79:8090–8097.
- Cooper CA, Gasteiger E, Packer NH. 2001. GlycoMod—A software tool for determining glycosylation compositions from mass spectrometric data. *Proteomics* 1:340–349.
- Cooper CA, Harrison MJ, Wilkins MR, Packer NH. 2001. GlycoSuiteDB: A new curated relational database of glycoprotein glycan structures and their biological sources. *Nucleic Acids Res* 29:332–335.
- Dell A, Morris HR. 2001. Glycoprotein structure determination mass spectrometry. *Science* 291:2351–2356.
- Didraga M, Barroso B, Bischoff R. 2006. Recent developments in proteoglycan purification and analysis. *Curr Pharm Anal* 2:323–337.
- Domon B, Costello CE. 1988. A systematic nomenclature for carbohydrate fragmentations in FAB-MS MS spectra of glycoconjugates. *Glycoconj J* 5:397–409.
- Dube DH, Bertozzi CR. 2005. Glycans in cancer and inflammation. Potential for therapeutics and diagnostics. *Nat Rev Drug Discov* 4:477–488.
- Ernst B, Muller DR, Richter WJ. 1997. False sugar sequence ions in electrospray tandem mass spectrometry of underivatized sialyl-Lewis-type oligosaccharides. *Int J Mass Spectrom Ion Processes* 160:283–290.
- Ethier M, Saba JA, Spearman M, Krokhn O, Butler M, Ens W, Standing KG, Perreault N. 2003. Application of the StrOligo algorithm for the automated structure assignment of complex N-linked glycans from glycoproteins using tandem mass spectrometry. *Rapid Commun Mass Spectrom* 17:2713–2720.
- Francel TJ, Fukuda EK, Mciver RT. 1983. A diffusion-model for non-reactive ion loss in pulsed ion-cyclotron resonance experiments. *Int J Mass Spectrom Ion Processes* 50:151–167.
- Franz AH, Lebrilla CB. 2002. Evidence for long-range glycosyl transfer reactions in the gas phase. *J Am Soc Mass Spectrom* 13:325–337.
- Fuster MM, Esko JD. 2005. The sweet and sour of cancer: Glycans as novel therapeutic targets. *Nat Rev Cancer* 5:526–542.
- Gabelica V, Rosu F, De Pauw E, Lemaire J, Gillet JC, Pouilly JC, Lecomte F, Gregoire G, Schermann JP, Desfrancois C. 2008. Infrared signature of DNA G-quadruplexes in the gas phase. *J Am Chem Soc* 130:1810–1811.
- Gaucher SP, Morrow J, Leary JA. 2000. STAT: A saccharide topology analysis tool used in combination with tandem mass spectrometry. *Anal Chem* 72:2331–2336.
- Gauthier JW, Trautman TR, Jacobson DB. 1991. Sustained off-resonance irradiation for collision-activated dissociation involving Fourier-transform mass spectrometry—Collision-activated dissociation technique that emulates infrared multiphoton dissociation. *Anal Chim Acta* 246:211–225.
- Goldberg D, Sutton-Smith M, Paulson J, Dell A. 2005. Automatic annotation of matrix-assisted laser desorption/ionization N-glycan spectra. *Proteomics* 5:865–875.
- Goldberg D, Bern M, Li BS, Lebrilla CB. 2006. Automatic determination of O-glycan structure from fragmentation spectra. *J Proteome Res* 5:1429–1434.
- Hakansson K, Hudgins RR, Marshall AG, O’Hair RAJ. 2003. Electron capture dissociation and infrared multiphoton dissociation of oligodeoxynucleotide dications. *J Am Soc Mass Spectrom* 14:23–41.
- Harvey DJ. 2001. Identification of protein-bound carbohydrates by mass spectrometry. *Proteomics* 1:311–328.
- Harvey DJ. 2005. Proteomic analysis of glycosylation: Structural determination of N- and O-linked glycans by mass spectrometry. *Expert Rev Proteomics* 2:87–101.
- Harvey DJ. 2006. Analysis of carbohydrates and glycoconjugates by matrix-assisted laser desorption/ionization mass spectrometry: An update covering the period 1999–2000. *Mass Spectrom Rev* 25:595–662.
- Harvey DJ. 2008. Analysis of carbohydrates and glycoconjugates by matrix-assisted laser desorption/ionization mass spectrometry: An update covering the period 2001–2002. *Mass Spectrom Rev* 27:125–201.
- Harvey DJ, Bateman RH, Green MR. 1997. High-energy collision-induced fragmentation of complex oligosaccharides ionized by matrix-assisted laser desorption/ionization mass spectrometry. *J Mass Spectrom* 32:167–187.
- Harvey DJ, Mattu TS, Wormald MR, Royle L, Dwek RA, Rudd PM. 2002. “Internal residue loss”: Rearrangements occurring during the fragmentation of carbohydrates derivatized at the reducing terminus. *Anal Chem* 74:734–740.
- Hitchcock AM, Yates KE, Costello CE, Zaia J. 2008. Comparative glycomics of connective tissue glycosaminoglycans. *Proteomics* 8:1384–1397.
- Hofmeister GE, Zhou Z, Leary JA. 1991. Linkage position determination in lithium-cationized disaccharides—Tandem mass spectrometry and semiempirical calculations. *J Am Chem Soc* 113:5964–5970.

- Hofstadler SA, Griffey RH, Pasa-Tolic L, Smith RD. 1998. The use of a stable internal mass standard for accurate mass measurements of oligonucleotide fragment ions using electrospray ionization Fourier transform ion cyclotron resonance mass spectrometry with infrared multiphoton dissociation. *Rapid Commun Mass Spectrom* 12:1400–1404.
- Ishihama Y. 2005. Proteomic LC-MS systems using nanoscale liquid chromatography with tandem mass spectrometry. *J Chromatogr A* 1067:73–83.
- Jebanathirajah JA, Pittman JL, Thomson BA, Budnik BA, Kaur P, Rape M, Kirschner M, Costello CE, O'Connor PB. 2005. Characterization of a new qQq-FTICR mass spectrometer for post-translational modification analysis and top-down tandem mass spectrometry of whole proteins. *J Am Soc Mass Spectrom* 16:1985–1999.
- Joshi HJ, Harrison MJ, Schulz BL, Cooper CA, Packer NH, Karlsson NG. 2004. Development of a mass fingerprinting tool for automated interpretation of oligosaccharide fragmentation data. *Proteomics* 4:1650–1664.
- Kirmiz C, Li BS, An HJ, Clowers BH, Chew HK, Lam KS, Ferrige A, Alecio R, Borowsky AD, Sulaimon S, Lebrilla CB, Miyamoto S. 2007. A serum glycomics approach to breast cancer biomarkers. *Mol Cell Proteomics* 6:43–55.
- Kosaka T, Yoneyama-Takazawa T, Kubota K, Matsuoka T, Sato I, Sakaki T, Tanaka Y. 2003. Protein identification by peptide mass fingerprinting and peptide sequence tagging with alternating scans of nano-liquid chromatography/infrared multiphoton dissociation Fourier transform ion cyclotron resonance mass spectrometry. *J Mass Spectrom* 38:1281–1287.
- Kovacic V, Hirsch J, Kovac P, Heerma W, Thomasoates J, Haverkamp J. 1995. Oligosaccharide characterization using collision-induced dissociation fast-atom-bombardment mass-spectrometry—Evidence for internal monosaccharide residue loss. *J Mass Spectrom* 30:949–958.
- Lancaster KS, An HJ, Li BS, Lebrilla CB. 2006. Interrogation of N-linked oligosaccharides using infrared multiphoton dissociation in FT-ICR mass spectrometry. *Anal Chem* 78:4990–4997.
- Li WQ, Hendrickson CL, Emmett MR, Marshall AG. 1999. Identification of intact proteins in mixtures by alternated capillary liquid chromatography electrospray ionization and LC ESI infrared multiphoton dissociation Fourier transform ion cyclotron resonance mass spectrometry. *Anal Chem* 71:4397–4402.
- Little DP, Aaserud DJ, Valaskovic GA, McLafferty FW. 1996. Sequence information from 42–108-mer DNAs (complete for a 50-mer) by tandem mass spectrometry. *J Am Chem Soc* 118:9352–9359.
- Lohmann KK, von der Lieth CW. 2004. GlycoFragment and Glyco-SearchMS: Web tools to support the interpretation of mass spectra of complex carbohydrates. *Nucleic Acids Res* 32:W261–W266.
- Ma YL, Vedernikova I, Van den Heuvel H, Claeys M. 2000. Internal glucose residue loss in protonated O-diglycosyl flavonoids upon low-energy collision-induced dissociation. *J Am Soc Mass Spectrom* 11:136–144.
- Ma B, Simala-Grant JL, Taylor DE. 2006. Fucosylation in prokaryotes and eukaryotes. *Glycobiology* 16:158r–184r.
- Maass K, Ranzinger R, Geyer H, von der Lieth CW, Geyer R. 2007. “Glycopeakfinder”—de novo composition analysis of glycoconjugates. *Glycobiology* 17:4435–4444.
- Marzluff EM, Campbell S, Rodgers MT, Beauchamp JL. 1994. Low-energy dissociation pathways of small deprotonated peptides in the gas-phase. *J Am Chem Soc* 116:7787–7796.
- Mechref Y, Novotny MV, Krishnan C. 2003. Structural characterization of oligosaccharides using MALDI-TOF/TOF tandem mass spectrometry. *Anal Chem* 75:4895–4903.
- Mirgorodskaya E, O'Connor PB, Costello CE. 2002. A general method for precalculation of parameters for sustained off resonance irradiation/collision-induced dissociation. *J Am Soc Mass Spectrom* 13:318–324.
- Park YM, Lebrilla CB. 2005. Application of Fourier transform ion cyclotron resonance mass spectrometry to oligosaccharides. *Mass Spectrom Rev* 24:232–264.
- Peiris DM, Riveros JM, Eyley JR. 1996. Infrared multiple photon dissociation spectra of methanol-attached anions and proton-bound dimer cations. *Int J Mass Spectrom Ion Processes* 159:169–183.
- Perez S, Mulloy B. 2005. Prospects for glycoinformatics. *Curr Opin Struct Biol* 15:517–524.
- Pikulski M, Hargrove A, Shabbir SH, Anslyn EV, Brodbelt JS. 2007. Sequencing and characterization of oligosaccharides using infrared multiphoton dissociation and boronic acid derivatization in a quadrupole ion trap. *J Am Soc Mass Spectrom* 18:2094–2106.
- Powell AK, Harvey DJ. 1996. Stabilization of sialic acids in N-linked oligosaccharides and gangliosides for analysis by positive ion matrix-assisted laser desorption ionization mass spectrometry. *Rapid Commun Mass Spectrom* 10:1027–1032.
- Rudd PM, Elliott T, Cresswell P, Wilson IA, Dwek RA. 2001. Glycosylation and the immune system. *Science* 291:2370–2376.
- Seipert RR, Dodds ED, Clowers BH, Beecroft SM, German JB, Lebrilla CB. 2008. Factors that influence fragmentation behavior of N-linked glycopeptide ions. *Anal Chem* 80:3684–3692.
- Stephens E, Maslen SL, Green LG, Williams DH. 2004. Fragmentation characteristics of neutral N-linked glycans using a MALDI-TOF/TOF tandem mass spectrometer. *Anal Chem* 76:2343–2354.
- Tang HX, Mechref Y, Novotny MV. 2005. Automated interpretation of MS/MS spectra of oligosaccharides. *Bioinformatics* 21:1431–1439.
- Tseng K, Hedrick JL, Lebrilla CB. 1999. Catalog-library approach for the rapid and sensitive structural elucidation of oligosaccharides. *Anal Chem* 71:3747–3754.
- Tsybin YO, Ramstrom M, Witt M, Baykut G, Hakansson P. 2004. Peptide and protein characterization by high-rate electron capture dissociation Fourier transform ion cyclotron resonance mass spectrometry. *J Mass Spectrom* 39:719–729.
- Varki A. 1993. Biological roles of oligosaccharides—All of the theories are correct. *Glycobiology* 3:97–130.
- Watson CH, Zimmerman JA, Bruce JE, Eyley JR. 1991. Resonance-enhanced 2-laser infrared multiple photon dissociation of gaseous-ions. *J Phys Chem* 95:6081–6086.
- Williams ER, Furlong JJP, McLafferty FW. 1990. Efficiency of collisionally-activated dissociation and 193-Nm photodissociation of peptide ions in Fourier-transform mass-spectrometry. *J Am Soc Mass Spectrom* 1:288–294.
- Wilson JJ, Brodbelt JS. 2006. Infrared multiphoton dissociation for enhanced de novo sequence interpretation of N-terminal sulfonated peptides in a quadrupole ion trap. *Anal Chem* 78:6855–6862.
- Wolff JJ, Chi LL, Linhardt RJ, Amster IJ. 2007. Distinguishing glucuronic from iduronic acid in glycosaminoglycan tetrasaccharides by using electron detachment dissociation. *Anal Chem* 79:2015–2022.
- Wuhrer M, Catalina MI, Deelder AM, Hokke CH. 2007. Glycoproteomics based on tandem mass spectrometry of glycopeptides. *J Chromatogr B Anal Technol Biomed Life Sci* 849:115–128.
- Wysocki VH, Kentamaa HI, Cooks RG. 1987. Internal energy-distributions of isolated ions after activation by various methods. *Int J Mass Spectrom Ion Processes* 75:181–208.
- Xie YM, Lebrilla CB. 2003. Infrared multiphoton dissociation of alkali metal-coordinated oligosaccharides. *Anal Chem* 75:1590–1598.
- Xie YM, Tseng K, Lebrilla CB, Hedrick JL. 2001. Targeted use of exoglycosidase digestion for the structural elucidation of neutral O-linked oligosaccharides. *J Am Soc Mass Spectrom* 12:877–884.
- Zaia J, Costello CE. 2003. Tandem mass spectrometry of sulfated heparin-like glycosaminoglycan oligosaccharides. *Anal Chem* 75:2445–2455.
- Zhang JH, Lindsay LL, Hedrick JL, Lebrilla CB. 2004. Strategy for profiling and structure elucidation of mucin-type oligosaccharides by mass spectrometry. *Anal Chem* 76:5990–6001.
- Zhang JH, Schuboth K, Li BS, Russell S, Lebrilla CB. 2005. Infrared multiphoton dissociation of O-linked mucin-type oligosaccharides. *Anal Chem* 77:208–214.